J. Nano- Electron. Phys.
3 (2011) No1, P. 453-459

© 2011 SumDU
(Sumy State University)

PACS numbers: 75.50.Pp, 71.20.Nr, 75.50.Dd, 61.72.uj, 81.05.Dz

FERROMAGNETISM IN NITROGEN DOPED MAGNESIUM OXIDE: A FIRST PRINCIPLE STUDY

V. Sharma, J.E. Lowther

School of Physics and DST/NRF Centre of Excellence in Strong Materials,
University of the Witwatersrand, Johannesburg, 2050 South Africa
E-mail: vinit.sharma.mlsu@gmail.com

The formation of magnetic moment in the p-orbital doped semiconductors is named d^0 magnetism, where the ion without partially filled d states is found to be responsible for the magnetism. To study origin of magnetism in such p-orbital doped semiconductors, we report a theoretical investigation of electronic and magnetic properties of N doped MgO, with and without an oxygen vacancy. The first principle calculations have been performed using ab initio total energy calculations with in generalized gradient approximation (GGA) as embodied in projector augmented wave (PAW) method. Our results suggest that without other defects, the oxygen vacancy does not reflect magnetism. It is observed that when N, substitutes for oxygen, it shows spontaneous magnetization and affect the magnetic moment of dopant. Although, the total magnetic moment of the system is independent of the presence of oxygen vacancies and found to be 1 *μB.*

Keywords: *NONMETALLIC FERROMAGNETIC MATERIALS, FIRST PRINCIPLE CALCULATIONS, MAGNETIC SEMICONDUCTORS, DENSITY FUNCTIONAL THEORY, WIDE BAND GAP SEMICONDCUTORS.*

(Received 04 February 2011, in final form 15 June 2011)

1. INTRODUCTION

In recent years, intensive research effort has been devoted to the search of materials with semiconducting properties and ferromagnetism at room temperature. New materials must be found that satisfy different types of requirements like high spin polarization or high Curie temperature. The search for stable half-metallic ferromagnets and ferromagnetic semiconductors with Curie temperatures higher than room temperature has led to intense research in the field of Dilute magnetic semiconductors (DMSs). Dilute magnetic semiconductors (DMSs), particularly based on III-V and II-VI hosts, have been studied due to their potential application in various spintronic devices such as spin-resonant tunneling diodes, spin light emitting diodes [1-2], etc. DMSs compounds can be made as half-metals, showing a high spin polarization of the conduction electrons of up to 100% in magnetic tunnel junctions. Several nitrides, arsenides and oxides, such as GaN, AlN, InN, GaAs, TiO_2, SnO_2, In_3O_3, HfO_2, and ZnO, have been investigated and found to exhibit ferromagnetism when doped with transition metal impurities [3-7].

For dilute magnetic semiconductors, it is found that the substitution of anion with an atom of smaller valency, introduces spin polarized gap states. Oxides doped with light elements have received considerable interest as efficient photoactive materials. Electronic paramagnetic resonance experiments have also

shown that the doping of light elements induce magnetic defect centers in the bulk material [8, 9].

In the search of new ferromagnetic materials, cation vacancy induced ferromagnetic ordering in CaO was reported by Elfimov et al. [10]. It is also observed that the presence of light element impurities (such as B, C, or N), in same compound, also contain a magnetic moment at the dopant site [11]. Furthermore, the ferromagnetism is also observed experimentally as well as theoretically in N doped SrO [12]. Butler et al. [13] and Mathon and Umerski [14], have predicted a high magnetoresistance (MR) ratio using first principle calculations and followed by the experimental evidence of magnetic tunnelling junctions with MgO single crystals as tunnelling barriers [15, 16]. It is therefore of interest to investigate the effect of doping main group elements in the presence as well as absence of oxygen vacancy, in order to understand the mechanism of ferromagnetism in MgO based dilute magnetic semiconductors.

MgO, which crystallizes in the rock-salt structure, is of huge interest as a tunnelling barrier in spintronics applications. Recently, it is reported that in such tunnelling process MgO single crystal only allows half-metallic Blochl states with Δ_1 symmetry to pass, leading to the giant magneto resistance effect [17]. On the other hand, If MgO is made ferromagnetic via dilute magnetic doping, it may also work as a spin filter [18] as well as induce a large magnetic-field effect [19]. Up to now, a considerable work has also been reported on the magnetism of metal [20-24] non-metal [25-28] element doping in the magnesium oxide.

In this work we perform a first principle calculation to study magnetic effects in MgO. In particular we investigated the role played by defects in origin of ferromagnetism in such wide band gap semiconductors.

2. COMPUTATIONAL DETAILS

Full structural optimization and electronic properties calculations were performed employing the Vienna *ab initio* simulation package (VASP) [29, 30] with the projector augmented plane wave basis functions [31, 32]. The exchange-correlation interaction was treated within the generalized gradient approximation (GGA) using the PW91 functional. The total energy was minimized by calculating of Hellmann-Feynman forces and the stress tensor. Relaxation of atomic positions and optimization of lattice parameters have been done by the conjugate gradient method. The electronic wave functions were expanded in the plane waves up to a cut-off energy of 500 eV, atomic relaxation was stopped when forces acting on atoms were less than 0.01 eV/Å. The total energy was converged to less than 0.001 eV/atom and 8Ч8Ч8 grid of Monkhorst-Pack points was used. The pseudopotentials based on the projector augmented wave method explicitly include the O (2*s* and 2*p*), Mg (3*s* and 3*p*), C (2*s* and 2*p*) and Mn (3*p*, 4*s* and 3*d*) electrons in the valence states. The total and projected DOS have been calculated by the linear tetrahedron method with Bloch corrections [33].

In the present study, a $2 \times 2 \times 2$ supercell containing 64 atoms is considered for all calculations. A representative structure diagram corresponding to all studied systems is shown in Figure 1. In Fig. 1, positions of host atoms (Mg and O) and dopant (N) along with oxygen vacancy is labeled. The lattice parameters a, based on minimization of the energy of the perfect lattice, was calculated to be $a = 8.4733$ Å.

To examine the stability of the formation of these defects, For all configurations, the formation energies of the defects were determined according to this formula

$$E^{p} = E_{tot}^{D} - E_{tot}^{B} \pm \sum n_i \mu_i$$

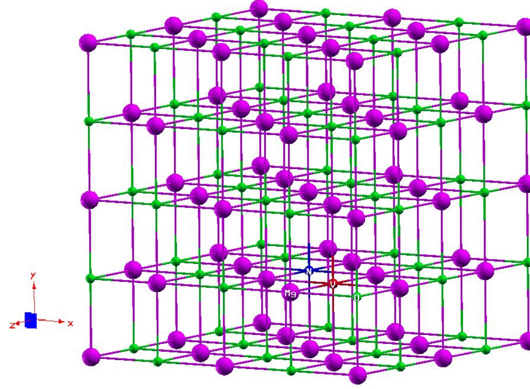

Fig. 1 *– Schematic structure diagram for the 2 × 2 × 2 supercell of MgO, positions of the host atoms (Mg and O), dopant (N) and oxygen vacancy (v) is labeled*

where E_{tot}^{D} is the total energy of the fully relaxed supercell containing a vacancy, E_{tot}^{B} is the total energy of the ideal supercell and n is the number of atoms and μ is the chemical potential. (+) and (–) sign are corresponds to atoms added and removed in the host lattice, respectively. If the formation energy is calculated in the infinite crystal, The chemical potentials of the removed atoms were calculated using the chemical potentials of the O_2 molecule.

3. RESULTS AND DISCUSSION

In the first set of calculations, we have considered a neutral O vacancy in the $2 \times 2 \times 2$ supercell by removing one O atom, for the position of O vacancy as shown in Fig. 1. The oxygen vacancy results two extra electrons in the supercell. These extra electrons show neither valence band nor conduction band character as they occupy a symmetric orbital. Therefore, the neutral O vacancy does not reflect any ferromagnetism. The formation energy for this case suggests that the presence of O vacancy in this semiconductor is feasible. But the spin polarization energy shows that the spin polarization states do not favor over the non-spin polarization states. Values of the formation energy, spin polarization energy along with magnetic moment of other studied configurations are given in Table 1.
To explore the electronic properties in Figures 2 a-c, the calculated total and partial spin resolved density of states (DOS) for MgO in the presence of oxygen vacancy, are shown. It is clear from Fig. 2 that the spin polarized DOS for O vacancy in MgO are all most identical for spin up and spin down states. When substituting O, N induces p states in the MgO gap, approximately in the range of 0.5 eV near the valence band edge. As N is electron efficient than O, the gap states host one unpaired hole, resulting a magnetic moment of 1 μB per N atom.

***Table 1** – The calculated formation energy, spin polarization energy and magnetic moments for various defect configuration of MgO*

System	Formation Eng. (eV)	Spin Pol. Eng. (eV)	Magnetic Moment (μB)			
			Dopant			supercell
MgO with			s	p	tot	Total
O Vac.	6.94	0.000017				
N_O-doping	10.04	– 0.10828	0.025	0.697	0.722	1.004
N_O with O_{vac}	15.69	– 0.17744	0.020	0.531	0.551	1.000

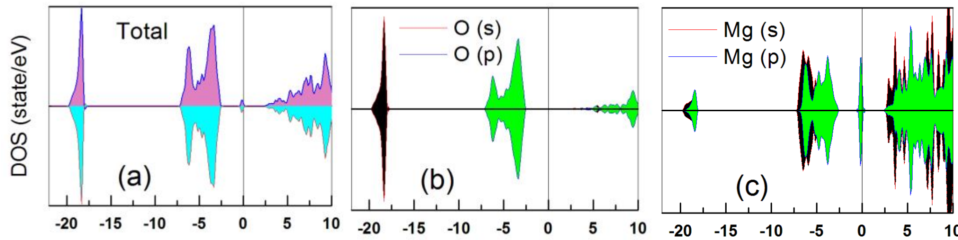

***Fig. 2** – Spin resolved density of states of MgO in the presence of oxygen vacancy (a) total (b) O and (c) Mg*

The same value of magnetic moment was calculated for N doped MgO in the presence of oxygen vacancy. The position of vacancy (where from the single O atom was removed from the supercell) is labeled in Fig. 1. For both the doping configurations, the results of magnetic moment along with formation energy and spin polarization energy are listed in Table 1. The formation energy for both the doping configurations suggests that such doping is energetically favorable and feasible. Moreover, on the basis of total energy calculations, it is also observed that, for N doped MgO, the spin-polarized state favours over the non-spin-polarized state by 108 (177) 177 meV in the absence (presence) of oxygen vacancy.

In order to obtain a unified picture of the nitrogen defects in MgO, we have calculated the total and partial DOS. The DOS for both the defect configurations, without and with the oxygen vacancy are shown in Fig. 3 (a-d) and 4 (a-d), respectively. Figs. 3 and 4 depict that near the Fermi level (E_F), there is a strong coupling between 2*p* states of N, O. The main feature indicated in the DOS figures is the hole states located around E_F, which are mainly arise due to the N (2*p*) and O (2*p*) states. The density of states also reveals that the hybridization between N dopant and its neighboring host atoms (Mg and O) results in the splitting of the energy levels near the E_F, which shifts the majority-spin states downward and minority-spin states upward to lower the total energy of the system, indicating the ideal case for spin injection applications due to 100 % spin-polarized carriers.

The impurity bands introduced by the N dopants occupy the energy level above the valence band maximum, which shows that the doped N atoms can induce the MgO to *p*-type semiconductor. Since, in both the cases, the majority-spin bands are fully occupied while the minority-spin bands are

partially filled, the number of holes in the system is equal to the magnetic moment, 1.0 μB per supercell. The magnetic moments are mainly contributed by the 2*p* states of N orbital (0.70 μB/N) and (0.53 μB/N) in the presence and absence of oxygen vacancy, respectively. The nearing neighbours Mg atom contributes 0.004 μB, and second neighbouring O atom provides 0.08 μB. The magnetic moments of the atoms have the same direction, indicating there is FM coupling between the doped N atom and neighbouring host atoms, which is similar with the results of N-doped ZnO [34].

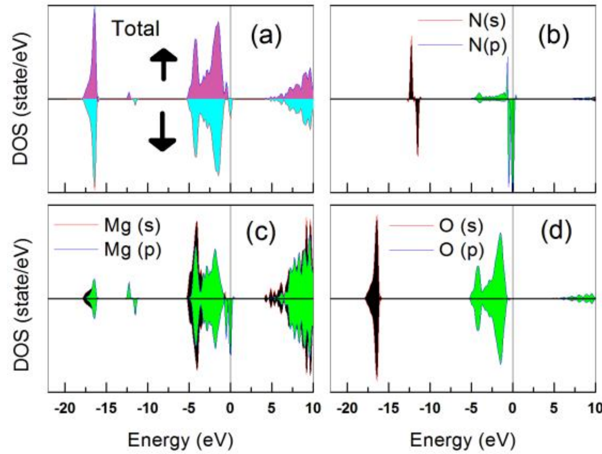

Fig. 3 *– Spin resolved total and partial density of states of N doped MgO in the absence of oxygen vacancy (a) total, (b) dopant N, (c) host Mg, and (d) host atom O*

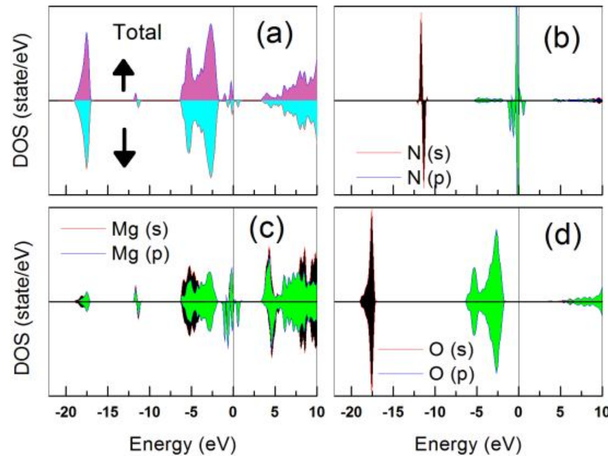

Fig. 4 *– Spin resolved total and partial density of states of N doped MgO in the presence of oxygen vacancy (a) total (b) dopant N, (c) host Mg and (d) host atom O*

To discuss the FM coupling further, in Fig. 5 a-c the spin-density plots for all studied configurations also shown. It is evident from the Fig. 5a, that the presence of oxygen vacancy in in bulk MgO doesn't leads to any magnetism. While in other two cases, the spin-polarized holes is localized

mainly on the N atom and distributed slightly over its four first nearing Mg atoms and the second nearing O atoms. These results clearly indicate thatthat the magnetic coupling clearly extends to the second nearing O atoms from the N dopant position. Therefore, it can be concluded that anions from the delocalized *p* orbitals contribute to the magnetic moment in N doped MgO.

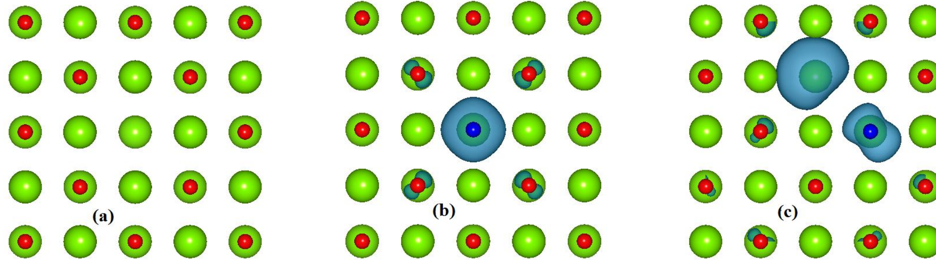

Fig. 5 *– The spin-density plot of (a) MgO with oxygen vacancy (b) N doped MgO and (c) N doped MgO in the presence of oxygen vacancy. The green, red, and blue balls represent the Mg, O and N, respectively.*

Furthermore, to explore the effect of oxygen vacancy in the magnetism of N doped MgO, the in spin density plot is presented in Fig. 5 (c). Although the presence of oxygen vacancy doesn't affect the total magnetism of the system but the presence of oxygen vacancy share a major contribution in total moment along with dopant (N).

This is also evident from the Fig. 5 (c), where it is can be seen that the holes localized around the position of oxygen vacancy are polarized. These polarized holes mediate the strong coupling between the oxygen vacancy and the N atoms.

4. CONCLUSIONS

In summary, In conclusion, we investigated the effects of electron doping on the magnetic moment formation of N doped MgO. For this, the first-principle density functional theory calculations are performed in both presence and absence of oxygen vacancy. From the defects studied we have found the only oxygen vacancy doesn't show any magnetism. But, it is found that the doping of N results a strong coupling between 2*p* states of dopant (N) and host (O). We find that for both doping concentrations the impurity levels are deep in the MgO gap and the magnetic moment is stable against the presence of oxygen vacancy. However, lattice distortion always promotes the localization of the doping hole, thus reducing the chance of long range magnetic coupling between impurities.

We acknowledge the support from the DST/NRF Center of Excellence in strong materials, South Africa.

REFERENCES

1. H. Ohno, *Science* **281,** 951 (1998).
2. Y. Ohno, D.K. Young, B. Beschoten, F. Matsukura, H. Ohno D.D. Awschalom, *Nature* **402,** 790 (1999).
3. J.M.D. Coey, M. Venkatesh C.B. Fitzgereald, *Nat. Mater.* **4,** 173 (2005).
4. N.H. Hong, J. Sakai, N. Poirot A. Ruyter, *Appl. Phys. Lett.* **86,** 242505 (2005).
5. J. He, S. Xu, Y.K. Yoo, Q. Xue, H.C. Lee, S. Cheng, X.-D. Xiang, G.F. Dionne, I. Takeuchi, *Appl. Phys. Lett.* **86,** 052503 (2005).
6. N.H. Hong, J. Sakai, W. Prellier G.F.A. Hassini, *Phys. Rev. B* **72,** 045336 (2005).
7. M. Venkatesh, C.B. Fitzgerald, J.G. Lunney J.M.D. Coey, *Phys. Rev. Lett.* **93,** 177206 (2004).
8. S. Livraghi, M.C. Paganini, E. Giamello, A. Selloni, C.Di Valentin G. Pacchioni, *J. Am. Chem. Soc.* **128,** 15666 (2006).
9. W.E. Carlos, E.R. Glaser D.C. Look, *Physica B* **308,** 976 (2001).
10. I.S. Elfimov, S. Yunoki G.A. Sawatzky, *Phys. Rev. Lett.* **89,** 216403 (2002).
11. K. Kenmochi, M. Seike, K. Sato, A. Yanase, H. Katayama-Yoshida, *Jpn. J. Appl. Phys.* **43,** L934 (2004).
12. I.S. Elfimov, A. Rusydi, S.I. Csiszar, Z. Hu, H.H. Hsieh, H.J. Lin, C.T. Chen, R. Liang, G.A. Sawatzky, *Phys. Rev. Lett.* **98,** 137202 (2007).
13. W.H. Butler, X.G. Zhang, T.C. Schulthess J.M. MacLaren, *Phys. Rev. B* **63,** 054416 (2001).
14. J. Mathon, A. Umerski, *Phys. Rev. B* **63,** 220403 (2001).
15. S.S.P. Parkin, C. Kaiser, A. Panchula, P.M. Rice, B. Hughes, M. Samant, S.H. Yang, *Nature Mater.* **3,** 862 (2004).
16. S. Yuasa, T. Nagahama, A. Fukushima, Y. Suzuki, K. Ando, *Nature Mater.* **3,** 868 (2004).
17. L. Li, X. Fang, C. Zeng, *J. Phys. D: Appl. Phys.* **42,** 155003 (2009).
18. I. Zutirc, J. Fabian, D.S. Sarma, *Rev. Mod. Phys.* **76,** 323 (2004).
19. L. Esaki, P.J. Stiles, S. von Molnar, *Phys. Rev. Lett.* **19,** 852 (1967).
20. M. Pesci, F. Gallino, C.Di Valentin, G. Pacchioni, *J. Phys. Chem. C* **114,** 1350 (2010).
21. C. Erhammar, C.M. Araujo, K.V. Rao, S. Norgren, B. Johansson, R. Ahuja, *Phys. Rev. B* **82,** 134406 (2010).
22. D. Bang, T. Nozaki, Y. Suzuki1, K. Rhie, T.-S. Kim, A. Fukushima, S. Yuasa, E. Minamitani, H. Nakanishi H. Kasai, *J. Phys.: Conf. Series* **200,** 052004 (2010).
23. R. Valero, J.R.B. Gomes, D.G. Truhlar, F. Illas, *J. Chem. Phys.* **132,** 104701 (2010).
24. M.M. Ibrahim, Z. Feng, J.C. Dean, M.S. Seehra, *J. Phys.: Condens Matter* **4,** 7127 (1992).
25. G. Liu, S. Ji, L. Yin, G. Fei, C. Ye, *J. Phys.: Condens. Matter* **22,** 046002 (2010).
26. A. Droghettia, S. Sanvito, *Appl. Phys. Lett.* **94,** 252505 (2009).
27. K. Kenmochi, V.A. Dinh, K. Sato, A. Yanase, H. Katayama-Yoshida, *J. Phys. Soc. Jpn.* **73,** 2952 (2004).
28. S. Ho, S. Nobuki, N. Uemura, S. Mori, T. Miyake, K. Suzuki, Y. Mikami, M. Shiiki, S. Kubob, *J. Appl. Phys.* **106,** 014911 (2009).
29. G. Kresse, J. Hafner, *Phys. Rev. B* **49,** 14251 (1994).
30. G. Kresse, J. Furthmuller, *Comput. Mater. Sci.* **6,** 15 (1996).
31. G. Kresse, J. Furthmuller, *Phys. Rev. B* **54,** 11169 (1996).
32. G. Kresse, J. Joubert, *Phys. Rev. B* **59,** 1758 (1999).
33. P. Blochl, O. Jepsen, O.K. Andersen, *Phys. Rev. B* **49,** 16223 (1994).
34. H. Pan, J.B. Yi, L. Shen, R.Q. Wu, J.H. Yang, J.Y. Lin, Y.P. Feng, J. Ding, L.H. Van, J.H. Yin, *Phys. Rev. Lett.* **99,** 127201 (2007).